Final Scientific/Technical Report

DOE Award Number: DE-SC0021268
Name of Recipient: Regents of the University of Minnesota

Permeation Properties of Disordered Metal-Organic Framework Membranes Made by Vapor Phase Ligand Treatment

Tsapatsis (DE-SC0021212), J. Anibal Boscoboinik (DE-SC0021304), and Ilja Siepmann (DE- SC0021268)

Budget Period: 09/01/2020 – 08/31/2023

Principal Investigator: Michael Tsapatsis, lead-PI
J. Ilja Siepmann, PI at UMN, siepmann@umn.edu

Unlimited Distribution

Executive Summary

Zeolitic imidazolate frameworks (ZIFs) are nanoporous molecular sieves offering exciting opportunities for membrane- and adsorption-based gas separations. The Tsapatsis group developed an all-vapor-phase ligand induced permselectivation (LIPS) method for the fabrication of ZIF nanocomposite membranes. The LIPS method consists of a combination of atomic layer deposition of a dense oxide inside the mesopores of a porous support followed by transformation of the dense oxide deposit to nanoporous ZIF by exposure to sublimated vapors of an imidazolate ligand. It enables the formation of thin nanocomposite films consisting of ZIF deposited inside pores with diameters smaller than 10 nm. Vapor-phase conversion of the impermeable ZnO to ZIF increases flux of certain gases more than others. Vapor phase linker/ligand treatment (VPLT) can further modify the properties of LIPS and other membranes. The combination of LIPS with VPLT provides an all-vapor methodology for making and modifying ZIF membranes with the ability to control the ZIF deposit composition and the level of confinement in a variety of mesoporous supports. The propylene/propane separation performance of LIPS/VPLT ZIF membranes confined (entirely or partially) inside mesopores is remarkably superior to that of most conventional ZIF membranes consisting of unconfined (deposited on the external surface of porous supports) polycrystalline films.

The accomplishments of this award are: (i) understanding of the LIPS process using mathematical models of atomic layer deposition (ALD), (ii) development of surface modification methods (vapor, e-beam, plasma, and X-ray treatments) to tune permeation properties, (iii) microstructural control of ZIF-8 films using ALD (support modification, direct ALD, and by use of *in situ* permeability monitoring), (iv) molecular simulations, and (v) thin film characterization and adsorption measurements using spectroscopy.

This project has resulted in the publication of eight research articles and one review article, and the award has contributed to the training of two postdocs and four graduate students.

Introduction

Nanoporous materials (NPMs), including zeolites/zeotypes, metal-organic frameworks (MOFs), and covalent organic frameworks possess enormous potential in diverse areas relevant to the BES mission and objectives. ZIF-8, a zeolitic-imidazolate framework (ZIF) consisting of zinc (Zn) centers bridged by 2-methyl-imidazole (2mIm) ligands has been targeted for energy-efficient separation of small molecules. Disorder introduced ruing synthesis or post-synthetically has the potential to further increase the separation performance of ZIF-8.

The discovery of functional NPMs is directly related to numerous DOE Office of Science basic research needs (BRNs):

- *BRNs for the Hydrogen Economy*: "Needed breakthroughs in hydrogen storage technology will require **revolutionary new materials** … and obtain an **atomic- and molecular-level understanding** of the physical and chemical processes" and "**efficient, high-volume gas separations** are needed for preparing input gas streams, separating process gases, and purifying product streams."
- *BRNs for Carbon Capture*: "Highly **efficient and selective separation of small molecules or ions from complex mixtures** is a critical need … Novel approaches that use new materials and alternative driving forces have enormous potential for **dramatically reducing energy costs that currently hinder separation technologies**."
- National Academy *A Research Agenda for Transforming Separation Science*: "The biggest challenge in separation science is **understanding and designing for complex systems** … Areas where data science and predictive modeling and simulation can help advance separation science include 1) **solvation effects, solution structuring, and interfacial structure**; 2) thermodynamic separation mechanisms and molecular transport properties …"

The research targeting increasingly complex ZIF-8 materials and feed streams also aligns with the transformative opportunities in "Mastering Hierarchical Architectures and Beyond-Equilibrium Matter," "Beyond Ideal Materials and Systems: Understanding the Critical Roles of Heterogeneity, Interfaces, and Disorder," and "Achieving Revolutionary Advances in Models, Mathematics, Algorithms, Data, and Computing" highlighted in *Challenges at the Frontiers of Matter and Energy: Transformative Opportunities for Discovery Science, 2015 BES Advisory Committee*.

Background of the Collaboration

ZIF-8, a zeolitic-imidazolate framework (ZIF) consisting of zinc (Zn) centers bridged by 2-methyl-imidazole (2mIm) ligands has been targeted for propane/propylene separations due to a propylene diffusivity that is over 100 times greater than that of propane. Synthesis of high-quality ZIF membranes has been achieved by the Tsapatsis group using solvent-free deposition of ZnO layers that are then converted to ZIF by exposure to 2mIm. According to this process, which we call LIPS (ligand-induced perm-selectivation), the pores of an alumina support are first filled using atomic layer deposition (ALD) of an impermeable ZnO deposit that is then converted to a permeable and selective ZIF layer by exposure to 2mIm vapors. We also reported VPLT (Vapor-Phase Ligand Treatment) of ZIF-8 with 2-amino benzimidazole (2-abIm) to exchange 2mIm with 2-abIm and observed that the effective aperture size shifts upon exchange of 2mIm with 2-abIm to create a membrane that exhibits high selectivity for O_2/N_2 and other gas mixtures. This work set the stage for the ongoing collaborative work among Tsapatsis, Boscoboinik and Siepmann groups. The work supported by this award aims at further developing the LIPS and VPLT processes to create novel ZIF membranes confined (at least partially) within mesoporous supports. It also aims at fundamental understanding of how ZIF confinement in mesopores and ZIF/mesoporous support interfaces affect structural flexibility and permeation properties. A novel aspect of the proposed research is to use electron-beam (e-beam) modification of ZIF membranes to controllably alter their structure (e.g., causing amorphization and chemical modification) and permeation properties. To achieve this, a collaboration with the Fairbrother group (Chemistry, JHU) was initiated and enabled e-beam and X-ray irradiation of entire membranes.

ACCOMPLISHMENTS

The original GOALS of the proposed research, as stated in the proposal, are:

- Elucidate the role of the porous support structure on the confined growth of ZIF films.
- Extend the LIPS synthesis method and the VPLT modification approach to control membrane structure and permeation properties.
- Demonstrate the use of e-beam treatment for controlled amorphization and permeation property modification.
- Characterize the films made by LIPS and modified by VPLT and/or e-bam treatment using X-ray diffraction, X-ray photoelectron spectroscopy (XPS), and X-ray absorption near edge structure (XANES).
- Examine using molecular simulations the structure, adsorption, and permeation properties (under low and high sorbate loadings).

The following papers have been published:

[1] Angewandte Chemie Int. Ed., 60, 9316-9320, 2021, https://doi.org/10.1002/anie.202100173

[2] Chemical Communications, 57, 5250-5253, 2021, https://doi.org/10.1039/D1CC00252J

[3] AIChE Journal, 67, e17305, 2021, https://doi.org/10.1002/aic.17305

[4] Annual Review of Chemical and Biomolecular Engineering, 13, 529-555, 2022, https://doi.org/10.1146/annurev-chembioeng-092320-120148

[5] Nature Communications 13, 420, 2022, https://doi.org/10.1038/s41467-022-28050-z

[6] ACS Applied Materials & Interfaces, 14, 19023-19030, 2022, https://doi.org/10.1021/acsami.2c00259

[7] AIChE Journal, 68, e17889, 2022, https://doi.org/10.1002/aic.17889

[8] Journal of Chemical & Engineering Data 67, 1779-1771, 2022, https://doi.org/10.1021/acs.jced.2c00086

[9] Industrial & Engineering Chemistry Research, 62, 9335-9347, 2023, https://doi.org/10.1021/acs.iecr.3c01151

One additional manuscript is currently undergoing revisions:

M. Ahmad, R, Patel, D. T. Lee, P. Corkery, A. Kraetz, Prerna, S. A. Tenney, D. Nykypanchuk, X. Tong, J. I. Siepmann, M. Tsapatsis, J. A. Boscoboinik, "ZIF-8 vibrational spectra: Peak assignments and defect signals," ACS Applied Materials & Interfaces.

The accomplishments of this award are: (i) understanding of the LIPS process using mathematical models of ALD, (ii) development of surface modification methods (vapor, e-beam, plasma, and X-ray treatments) to tune permeation properties, (iii) microstructural control of ZIF-8 films using ALD (support modification, direct ALD, and by use of *in situ* permeability monitoring), (iv) molecular simulations, and (v) thin film characterization and adsorption measurements using spectroscopy. The direction of the project is following the original plan augmented with the addition of the activities performed by the Fairbrother group.

Modeling of Atomic Layer Deposition in Porous Media for Membrane Formation We completed the development of a mathematical model of thin film ZnO deposit formation by ALD in a mesoporous substrate. ZnO deposition in porous γ-Al_2O_3 via atomic layer deposition (ALD) is the critical first step for the fabrication of ZIF membranes using the LIPS process. Up to now, this step was performed empirically without quantitative understanding of the reactor design and operational parameters leading to uniform and thin deposits. A detailed Computational Fluid Dynamics (CFD) model of the ALD reactor used in the Tsapatsis group was developed using a finite-volume based code and validated. It accounts for the transport processes within the feeding system and reaction chamber and within the membrane support. The simulated precursor spatiotemporal profiles assuming no ALD reaction were used as boundary conditions in

modelling diethylzinc reaction/diffusion in porous γ-Al_2O_3, the predictions of which agreed with experimental electron microscopy measurements (**Figure 1**). The model also indicates that for typical laboratory-scale porous substrates (22 mm diameter), deposition takes place uniformly across the substrate, that is, differences in deposition rate and penetration depth between the leading and trailing edges of the substrate can be neglected ensuring a uniform deposit. This finding provides further confidence for the uniform microstructure of our membranes. Further simulations confirmed that the actual deposition flux (i.e., the flux attributed to the consumption of reactants as they diffuse and react in/on the substrate) is much less than the upper limit of flux, below which the decoupling of reactor/substrate is an accurate assumption. This greatly simplified the modeling of the ALD reactor and the formulation of the reaction/diffusion model of ZnO deposition within the porous support. The modeling approach demonstrated in this work is the first comprehensive modeling of ALD for membrane formation. It allows for the design of ALD processes for the synthesis of metal–organic framework membranes as well as other thin-film membranes in porous supports. This work was published in AIChE Journal, 67, e17305, 2021, https://doi.org/10.1002/aic.17305.

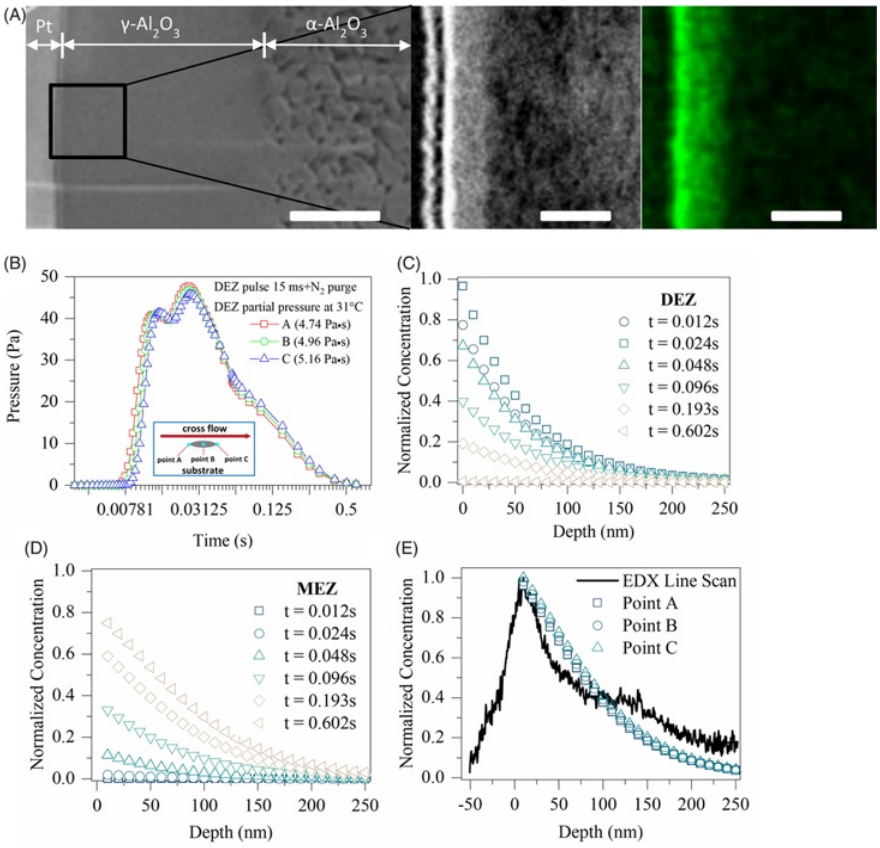

Figure 1. (A) Cross-section of a membrane with ZnO deposit, showing the macroporous α-Al_2O_3 and mesoporous γ-Al_2O_3 support, and higher magnification cross-sectional images of the ZnO deposit (bright contrast and green color) within the γ-Al_2O_3 layer (left scale bar: 1 μm, middle and right scale bars: 250 nm). (B) Transient diethylzinc (DEZ) boundary conditions determined by the atomic layer deposition reactor model (assuming no reaction) at three positions along the membrane (A, B, and C) as indicated in the inset. (C,D) Concentration profiles of DEZ and MEZ, respectively. (E) Final concentration profile of MEZ at positions *A*, *B*, and *C* compared to profile from cross-sectional imaging.

We extended our modeling effort considering the coexistence of atomic layer deposition (ALD) both inside the pores and on the outer surface of the substrate. Finite-volume based models were developed and validated to simulate the two distinct modes of deposition. The total mass uptake of the substrate with ALD cycles can be predicted using the combined surface deposition and pore reaction-diffusion models as affirmed by *in situ* quartz crystal microbalance experimental data (in collaboration with Professor Gregory Parsons, NC State). The ALD reactor model combined with the deposition model can accurately capture the number of ALD cycles needed to block the pores of the substrate. Based on the model, we designed a modified ALD process and examined the performance of the corresponding LIPS membranes.

Figure 2 shows characterization and membrane performance data for membranes prepared using the modified system. It was demonstrated that the modification allowed us to significantly increase the number

of ALD cycles to pore closure and provided much finer control of flux and selectivity of the obtained LIPS membranes. However, we were not able to improve the membrane performance from that exhibited by membranes prepared in the unmodified original ALD system. Our model revealed that penetration depth inside the substrate pores and external film thickness are similar in modified and unmodified systems at pore closure. This finding explains why the obtained LIPS membranes exhibit similar permeation behavior. *Our validated ALD model is now complete and can be used to examine the effect of operating conditions on deposit penetration depth and thickness.* This work was published in AIChE Journal, 68, e17889, 2022, https://doi.org/10.1002/aic.17889.

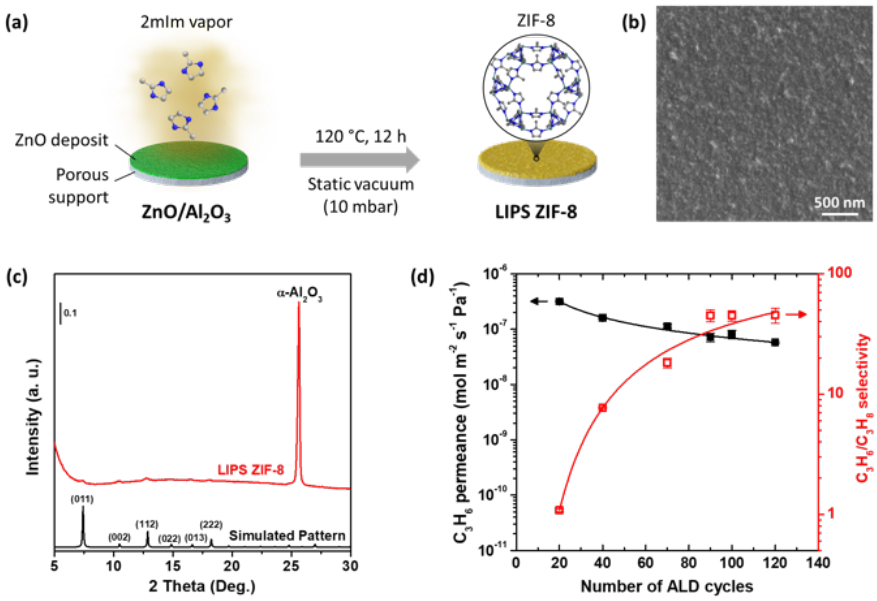

Figure 2. (a) Schematic of the LIPS ZIF-8 membrane synthesis process. The impermeable ZnO deposits on the mesoporous γ-Al_2O_3 layer are converted to ZIF-8 through 2-methylimidazole (2mIm) vapor treatment. (b) Top-view SEM image, (c) XRD pattern, and (d) propylene permeance and propylene/propane equi-molar feed mixture selectivity (at 25 °C) for LIPS ZIF-8 membranes formed from the porous support deposited with ZnO using orifice-modified gaskets.

ZIF-8 Membrane Modification

Vapor Phase Modification using Metal-Organic Precursors We demonstrated performance modification of ZIF-8 membranes based on a treatment using sublimated vapors of manganese (II) acetylacetonate. This work was motivated by earlier studies by others on transmetalation of ZIF-8 powders with redox-active manganese (II) in the liquid phase. Characterization of the modified ZIF-8 films and membranes using SEM, XRD and XPS support that $Mn(acac)_2$ treatment leads to formation of a thin top layer as opposed to metal doping or metal cation exchange with framework Zn, which was our original goal. The fact that, at the surface of the modified films, we detect by XPS N but not Zn indicates the presence of a layer that is not ZIF-8 but contains 2mIm ligands from the original ZIF-8 film. These 2mIm ligands are either bound to Mn or simply present within the $Mn(acac)_2$ layer. The thickness of the top layer can be estimated from XPS (i.e., based on the attenuation of the Zn 2p intensity from the underlying ZIF-8 film using as a reference the area of this core level peak prior to the $Mn(acac)_2$ treatment). It was found to be in range from 3 to 7 nm depending on the treatment temperature. We found that the 3 to 7 nm thick top layer drastically alters the permeation properties of the ZIF-8 membrane (**Figure 3**). Propylene/propane selectivity increases from 31 to 210 after the $Mn(acac)_2$ treatment at 165 °C for 30 min, while selectivities increase from 14.6 to 242 for H_2/CH_4, from 2.9 to 38 for CO_2/CH_4, from 2.4 to 29 for CO_2/N_2, and from 2.9 to 7.5 for O_2/N_2, after $Mn(acac)_2$ treatment at 175 °C for 30 min. Stable equimolar propylene/propane mixture selectivity of 165 at ambient temperature and 4 bar equimolar feed with a propylene flux of 8.3×10^{-4} mol m^{-2} s^{-1} was established. A control experiment excludes thermal treatment alone causing these changes.

Along with our earlier demonstration of vapor phase linker exchange, this work establishes vapor phase treatments with organic ligands and metal-organic precursors as a toolset for systematic manipulation of

membrane microstructure and composition. This work was published in Angewandte Chemie Int. Ed., 60, 9316-9320, 2021, https://doi.org/10.1002/anie.202100173.

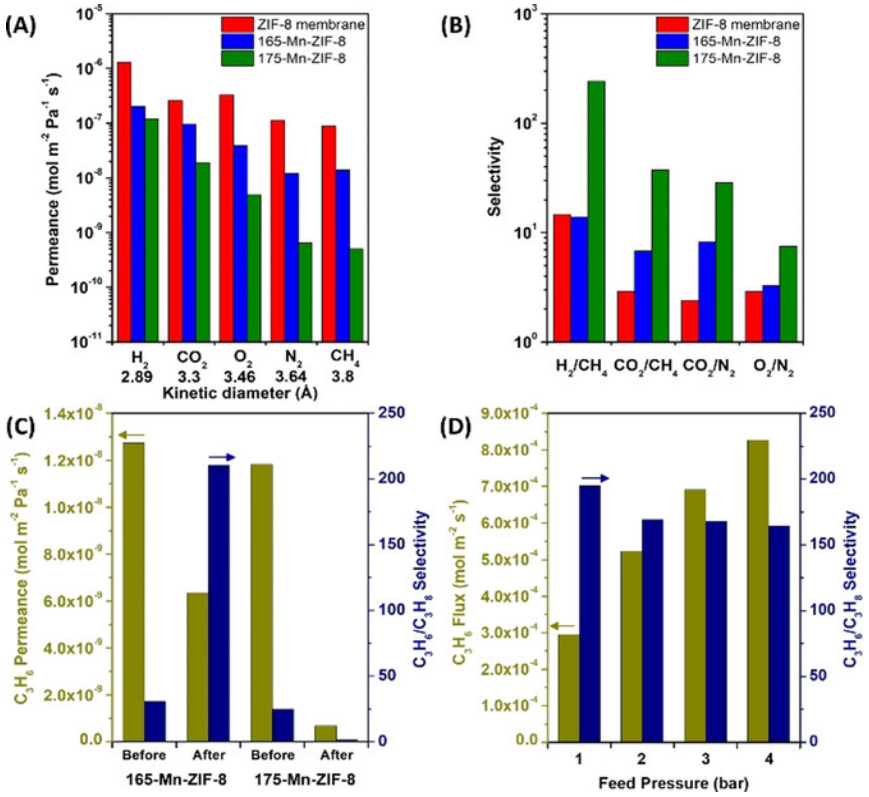

Figure 3. (A) Single gas permeances of H_2, CO_2, O_2, N_2, and CH_4, and (B) ideal selectivity (ratio of permeances) for H_2/CH_4, CO_2/CH_4, CO_2/N_2, and O_2/N_2 gas pairs measured at 25 °C by the time-lag method before and after $Mn(acac)_2$ treatment at 165 °C (165-Mn-ZIF-8) and 175 °C (175-Mn-ZIF-8). (C) Propylene permeance and propylene/propane equimolar feed mixture selectivity by the at 25 °C for 165- and 175-Mn-ZIF-8. (D) Propylene flux and propylene/propane selectivity (equimolar propane and propylene feed) for ZIF-8 membranes before and after $Mn(acac)_2$ treatment at 165 °C (165-Mn-ZIF-8) at feed (retentate) pressure ranging from 1 bar to 4 bar at 25 °C.

Electron-Beam Modification We proposed to explore electron-beam induced amorphization of ZIF-8 as a way to modify its permeation properties. This idea was based on our earlier studies of e-beam amorphization for patterned MOF formation.

For the patterning studies, we use a SEM to write patterns in a small (e.g., 5 μm x 5 μm area) of the ZIF film or on ZIF single crystals. For membrane formation, we need to be able to irradiate the entire membrane (ca. a disc with 22 mm diameter). This was a major challenge we faced, which we overcame by establishing a collaboration with the group of Professor Fairbrother (Chemistry, JHU) who was able to assemble a broad beam electron gun in his lab housed within a vacuum chamber. In this way, we were able to load and expose ZIF-8 membranes to an e-beam and then determine their properties after e-beam treatment.

Electron induced modification of MOFs has not been explored except for the well-documented beam damage problem in high-resolution microscopy and as a means for surface activation and functionalization. E-beam modification was accomplished by exposing the as-prepared LIPS membranes to the output of an electron flood gun operating at 2 kV.

We showed that electron irradiation can modify the gas permeation properties of a ZIF-8, as demonstrated by improved CO_2/N_2 and CO_2/CH_4 selectivity (**Figure 4**). Low dose exposure for less than 1 min increases CO_2 selectivity, while high dose exposure leads to reduced permeance and selectivity.

To investigate the changes caused by e-beam irradiation on the surface of ZIF-8, we collected XPS from ZIF-8 thin films irradiated by an *in situ* generated e-beam at Brookhaven National Lab. After irradiation, while no significant changes are observed in the binding energy of Zn 2p, a small shoulder appears at 401.2 eV in the N 1s spectrum. This change indicates the formation of N–H bonds due to the electron induced cleavage of either the Zn–N bond or the C–N/C═N bond in the imidazole ring. One possibility is that the breakage of bonds frees the transient nitrogen species to recombine with protons in a cascade of radical

reactions induced by the e-beam, and the presence of N–H bonds in open pores increases the adsorption of CO_2 in ZIF-8, leading to the improved CO_2 selectivity. At increased doses, crosslinking of imidazolate ligands could become dominant causing pore blocking and large reduction in flux.

Our work is the first use of e-beam irradiation for the modification of MOF membranes. This work was published in Chemical Communications, 57, 5250-5253, 2021, https://doi.org/10.1039/D1CC00252J

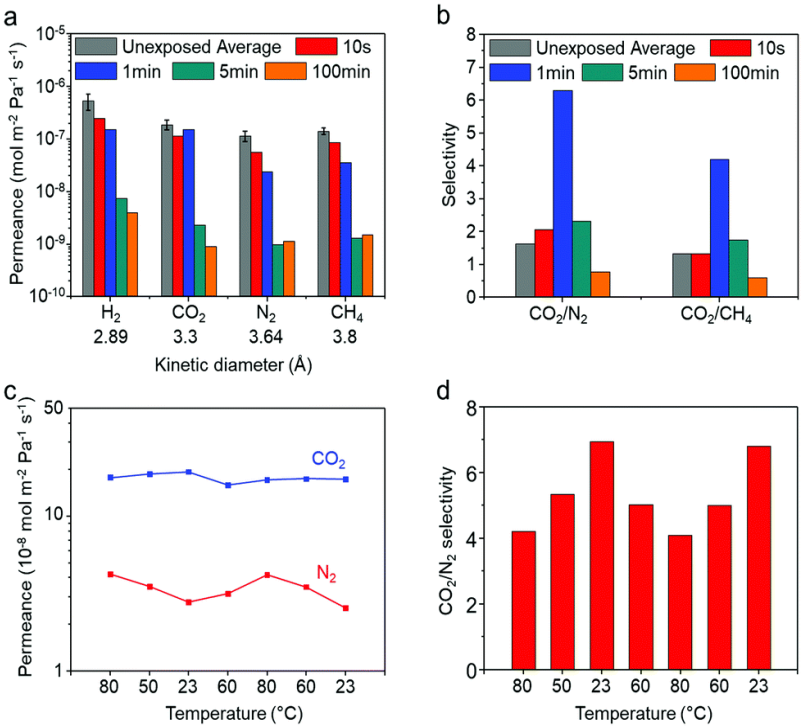

Figure 4. (a) Single gas permeances and (b) CO_2/N_2 and CO_2/CH_4 ideal selectivities of LIPS ZIF-8 membranes before and after e-beam exposure. (c) CO_2 and N_2 permeances at various temperatures in the 23–80 °C range of a membrane exposed to e-beam for 1 min, and (d) the corresponding ideal selectivities for CO_2/N_2. Permeances for each gas are measured over a period of 24 h at each temperature, respectively. The data points in (c) are from stabilized permeances with less than 10% variation in each on-stream stability test.

X-ray Modification We have demonstrated that in addition to e-beam irradiation as an external stimulus, membranes exposed to X-rays exhibit tunable modifications in the structure of the crystalline nanoporous layer and its gas permeation properties. Initially, we irradiated a ZIF-8 film (ca. 150 nm in thickness) (**Figure 5a**) with Mg K-alpha X-rays for 30 min. As shown in **Figure 5b**, X-ray diffraction (XRD) peak positions of the film were shifted towards higher 2-theta angles, and peak broadening and peak intensities decreased upon the X-ray exposure. This result denotes that the X-ray irradiation induces a decrease in the unit cell volume of ZIF-8, accompanied by increasing micro-strain. Furthermore, the contracted unit cell dimensions remain intact after heating at 120 °C for 2 h in air, as confirmed through XRD data (not included here) obtained after annealing.

We implemented the same X-ray treatment method to LIPS membranes to investigate the corresponding structural and permeation property changes. Interestingly, XRD patterns of X-ray-treated LIPS membranes (**Figure 5c**) reveal no detectable changes in peak position and intensity compared to untreated membrane counterparts, in marked contrast to the behavior of the freestanding ZIF-8 films (shown in **Figure 5a**, **b**).

It appears that the confined and disordered LIPS ZIF-8 membranes are more resistant to X-ray induced structural changes and/or that the changes cannot be detected due to the weak diffraction intensity of the LIPS membranes.

Moreover, in contrast to e-beam treatment discussed above, X-ray treatment does not cause permeance reduction for all gases (**Figure 9d**).

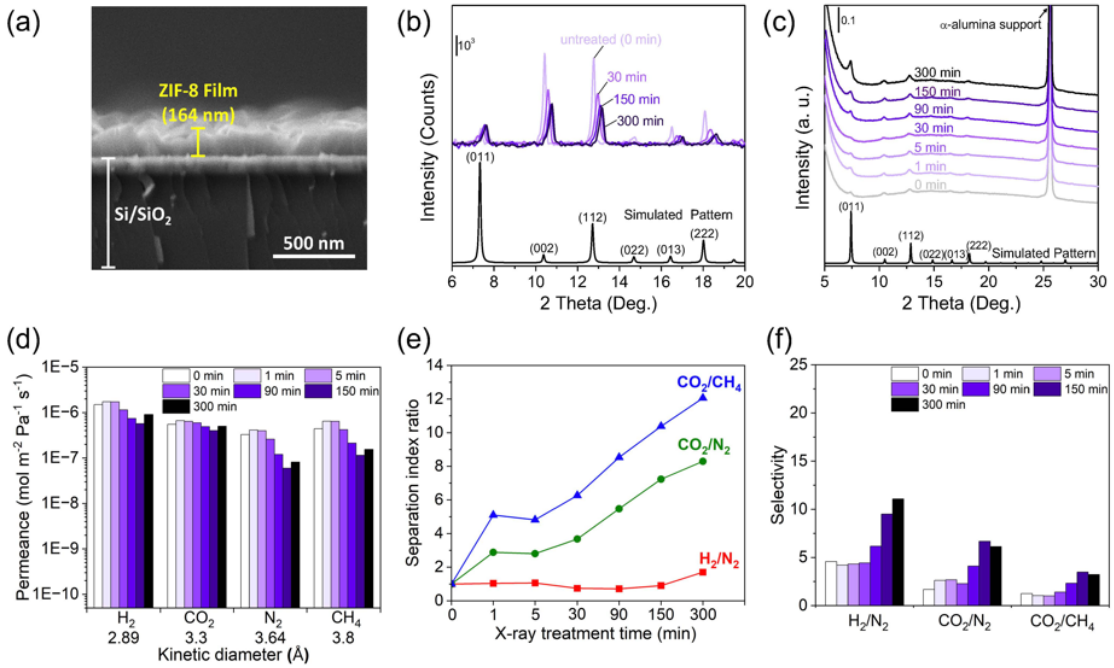

Figure 5. ZIF-8 modification by X-ray irradiation. (a) Cross-sectional SEM image of as-synthesized ZIF-8 film on a Si/SiO_2 substrate. (b) XRD patterns of the films before and after X-ray exposure (30 min). (c) XRD patterns of LIPS membranes before and after X-ray exposure (for 0 min to 300 min). (d) Single gas permeances of H_2, CO_2, N_2, and CH_4 measured at 25 °C by the time-lag method for LIPS ZIF-8 membranes before and after the X-ray exposure. (e) separation index ratios (Permeance(Selectivity-1) of membranes after X-ray treatment, divided by Permeance(Selectivity-1) of membranes before X-ray treatment) and (f) ideal selectivities (ratio of permeances) for H_2/N_2, CO_2/N_2, and CO_2/CH_4.

Most interestingly, although X-ray treatment of LIPS membranes does not result in any detectable changes in the XRD patterns, the X-ray treated LIPS membranes exhibit improved CO_2 selectivity without loss of CO_2 permeance (**Figures 5d**, **e**, **f**), which improves overall performance. A measure of membrane permeation performance that accounts for both permeance and selectivity is the separation index: the product of permeance (P) and selectivity (S) above one, P(S-1). The ratio of separation index for membranes after and before X-ray treatment (**Figure 5e**) shows that X-ray treatment can lead to 5- to 10-fold improvement in separation performance. This work is in preparation for submission.

These findings demonstrate that e-beam and X-ray irradiation can have distinct effects in membrane structure and performance. Moreover, they show that the effect of irradiation may vary depending on the initial microstructure of the membrane. Therefore, they justify further studies to elucidate the underlying phenomena responsible for the observed structure and permeation property changes.

Plasma Modification In addition to e-beam and X-ray treatments causing changes in selectivity, we reported that treatment of ZIF-8 membranes using mild non-thermal plasma (NTP) conditions yields a fivefold enhancement for H_2/N_2 and CO_2/CH_4 ideal selectivities and an eightfold enhancement for CO_2/N_2 ideal selectivity.

In this work, we combined the capabilities of infrared reflection absorption spectroscopy (IRRAS) with NTP for *in situ* interrogation of zeolitic imidazolate framework-8 (ZIF-8) thin films to probe modifications in the material induced by oxygen and nitrogen plasmas. **Figure 6a** shows IRRA spectra as a function of time during O_2 plasma exposure, while **Figure 6b** shows XPS spectra providing clear evidence of the formation of carbonyl groups as evidenced by a C 1s peak with a binding energy of 287.9 eV that appears and grows during the treatment. These changes are shown quantitatively in **Figure 6c** by tracking the areas

of the C 1s, O 1s, and N 1s core levels in XPS and the 1148 cm^{-1} framework phonon mode in IRRAS as a function of plasma treatment time. A more detailed analysis of the IRRAS data in oxygen plasma reveals the etching of organic ligands with sequential removal of the methyl group and imidazole ring and the formation of carbonyl moieties (C═O). In contrast, nitrogen plasma induces mild etching and grafting of nitrile groups (-C=N). Scanning electron microscopy imaging shows that oxygen plasma, at prolonged times, significantly degrades the ZIF-8 film at the grain boundaries. This is consistent with the fact that the enhancement in selectivity only takes place for short plasma treatments.

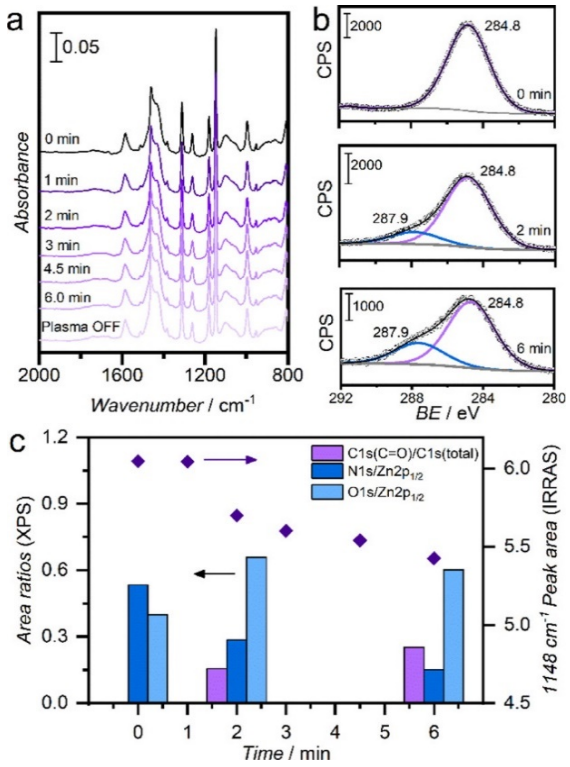

Figure 6. In situ tracking of ZIF-8 film treatment with O_2 plasma (10 W, 0.1 mbar O_2): (a) IRRA spectra; (b) high-resolution C 1s XPS spectra; (c) 1148 cm^{-1} peak area from IRRAS (diamonds), and element area ratios from XPS (bars).

This work showcases the development of novel surface science capabilities at the Center for Functional Nanomaterials of Brookhaven National Laboratory by this team enabling in situ *measurements during membrane modification.* It was published in ACS Applied Materials & Interfaces, 14, 19023-19030, 2022, https://doi.org/10.1021/acsami.2c00259.

Microstructure Control

Substrate Modification with Metal Nanoparticles for Nucleation and Growth Control In our effort to control ZIF-8 thin film microstructures, we studied the influence of metal nanoparticles (NPs) on the ZnO conversion to ZIF-8, and the integrity and position of the NPs in the final composite films. Our hypothesis was that metal nanoparticles will adsorb the imidazole vapors and alter the nucleation and growth kinetics. The effort to prepare ZIF-8 films with embedded metal nanoparticles is also motivated by their potential use to monitor transport of species like CO, which exhibit distinct spectroscopic signatures upon adsorption on metal surfaces, in the ZIF-8 film. Moreover, these embedded nanoparticles can lead to uses in practical applications including gas sensing and catalytic chemical transformations.

As shown in **Figure 7a-b**, densely packed Pd NPs were deposited *via* e-beam evaporation on the ZnO surface, which was made by ALD on a SiN transmission electron microscopy (TEM) grid. Two different types of surfaces were prepared on ZrO_2/Au/Si wafer substrates: i) Type I with Pd deposition on the ZnO surface and ii) Type II with ZnO deposition on top of the layer of Pd NPs (**Figure 7c**). A reflective Au film (100 nm in thickness) was deposited on a Si wafer to enhance the spectroscopic signals from infrared reflection absorption (IRRA). This arrangement is also appropriate for future *in situ* studies of gas adsorption. Furthermore, an approximately 15 nm-thick ZrO_2 layer was directly deposited on the Au surface to avoid any possible interaction of Au with overlayer components of ZnO and Pd NPs upon the subsequent ligand vapor treatment. Scanning electron microscope (SEM) images in **Figure 7c** present a clear difference in the morphology of the crystalline films formed upon the 2mIm vapor treatment: Type I leads to remarkably thicker and larger grains, while well-intergrown smaller crystals are formed from Type II as is typical for ZIF films transformed from bare ZnO with no metal components.[71] Grazing incidence X-ray diffraction (GIXD) in **Figure 7d** reveals that the crystalline species produced from Type I and Type II are

ZIF-8. Further studies are underway to determine the crystallographic orientation and internal microstructure of the large-gran deposits.

This work shows that the presence of metal nanoparticles on the support surface can drastically alter the nucleation and growth kinetics of ZIF-8 films made by the LIPS process and lead to novel microstructures. Since membrane supports (like porous alumina, which is typically used as a LIPS membrane support) can be functionalized with metal nanoparticles, these findings open new directions for optimizing ZIF membrane microstructure and performance. This work is in preparation for submission.

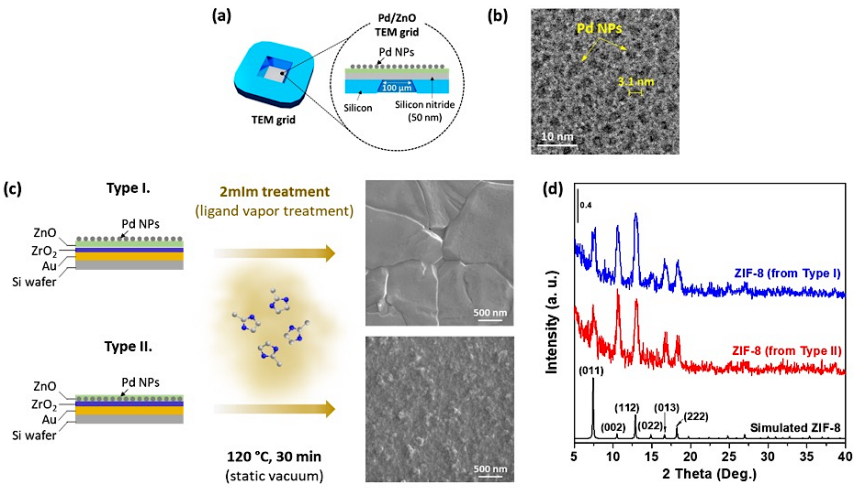

Figure 7. (a) Schematic illustration of the sample preparation on a 50 nm-thick silicon nitride (SiN) window for TEM analysis. (b) TEM image of Pd nanoparticles (NPs) deposited (electron-beam physical vapor deposition) on 13 nm-thick ZnO layer, atomic layer deposited on SiN surface. (c) Experimental procedure of the ZIF film growth in the presence of Pd NPs and top-view SEM images of the final products. (d) GIXD patterns of the final film products in (c).

Direct Deposition of Amorphous ZIFs and ZIF-8 Films (without formation of ZnO film) We developed an alternative ZIF film deposition method, which avoids the formation of an intermediate ZnO deposit (**Figures 8** and **9**). We anticipated that the microstructure of the directly-deposited films will be different from those obtained by LIPS because the large volume expansion (ca. 15-fold) associated with the ZnO to

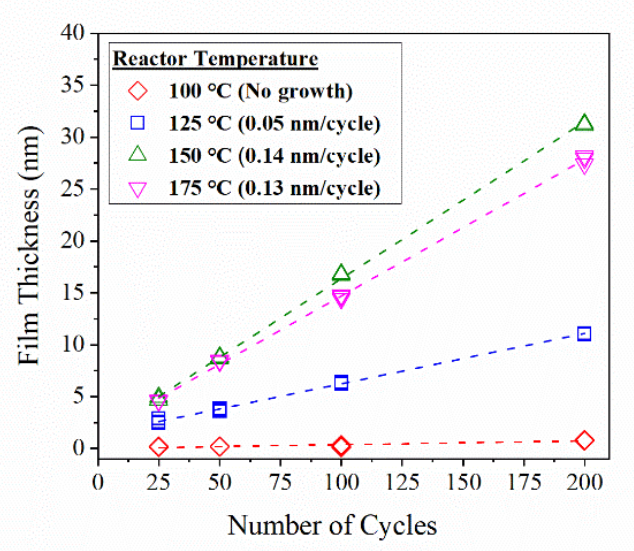

Figure 8. Film thickness of directly-deposited amorphous ZIF films (determined by ellipsometry) as a function of number of ALD cycles at different deposition temperatures.

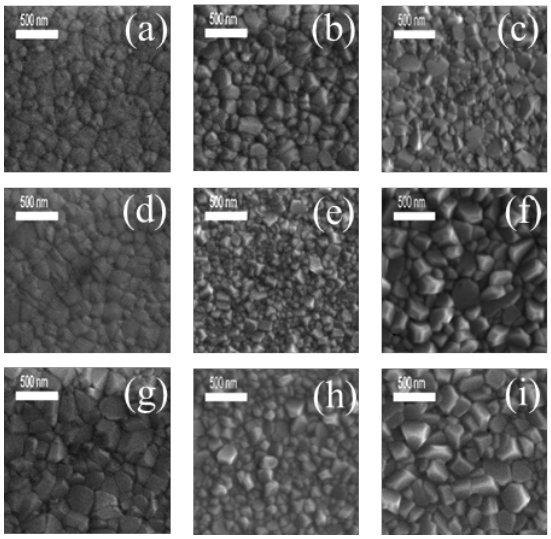

Figure 9. SEM images of ZIF-8 films formed by treatment of directly-deposited amorphous ZIFs with 2mIm vapors at 80 °C for (a) 30 min, (b) 1 h, (c) 4 h, 100 °C for (d) 30 min, (e) 1 h, (f) 4 h, and 120 °C for (g) 30 min, (h) 1 h, and (i) 4 h.

ZIF-8 transformation will be avoided. Moreover, we anticipated that direct deposition would allow formation of amorphous films avoiding the need to first form and then amorphize ZIF-8 films.

Amorphous zinc-imidazolate films were deposited on silicon wafers using an ALD/MLD recipe with alternating pulses of diethylzinc (DEZ) and 2mIm at temperatures of 125 to 175 °C. DEZ and 2mIm were pulsed sequentially into a home-built flow-through ALD reactor with intermittent argon gas purges to remove byproducts and unreacted precursors.

For crystallization of the amorphous zinc-imidazolate films deposited by ALD/MLD to ZIF-8, vapor phase treatments with 2mIM were performed at 80, 100, or 120 °C for 30 minutes, one hour, or four hours under static vacuum. Ellipsometry data demonstrate that growth of the amorphous zinc-imidazolate films is linearly related to number of deposition cycles, as expected for inorganic-organic thin films grown by ALD/MLD (**Figure 8**). Following exposure to 2mIm vapors in a batch system XRD data demonstrate conversion to crystalline ZIF-8 (**Figure 9**). Crystallinity developed faster at higher temperature, as expected due to the higher vapor pressure of 2mIm and the faster reaction kinetics. Following 2mIm vapor treatment, performed in a batch system at 80 °C or greater, SEM images reveal the formation of crystals in all samples.

This work demonstrates direct deposition of amorphous ZIF films and their subsequent transformation to crystalline ZIF-8, eliminating the formation of an intermediate ZnO layer. It is anticipated to enable novel membrane microstructures with yet unknown permeation properties. It is in preparation for submission.

In Situ Monitoring of Membrane Permeation During ZIF Film Formation and Modification We have designed and built a flow reactor system (shown in **Figure 10**, left) to measure the *in situ* permeance of an inert gas through a membrane as ZnO deposits are converted to a permeable layer by exposure to 2mIm vapors. This system can also be used for vapor phase modification treatments including the use of imidazolate and organometallic vapors. We have found that water vapor must be present to fully convert the ZnO to a permeable layer and that the reaction is aided by using a 2mIm vapor stream that is saturated or supersaturated at deposition conditions.

As shown in **Figure 10** (right), a slow decrease in permeance is observed for the first several hours of a treatment, possibly due to swelling of ZnO as 2mIm is incorporated into the deposits. This is followed by an increase in the permeance of greater than an order of magnitude that typically occurs in less than one hour. If the treatment is stopped at this point, the permeance will decrease again as shown in the red curve in **Figure 10**, likely due to rearrangements of 2mIm molecules in the membrane. If the treatment is continued, as shown in the black curve in **Figure 10**, the permeance will level off at a higher value. This set up can be used to monitor permeation changes during vapor deposition and modification of ZIF films.

This demonstration highlights the potential to monitor permeation during vapor (and possibly irradiation) treatments, directly linking membrane processing to function, allowing for precisely controlling processing for achieving optimized performance.

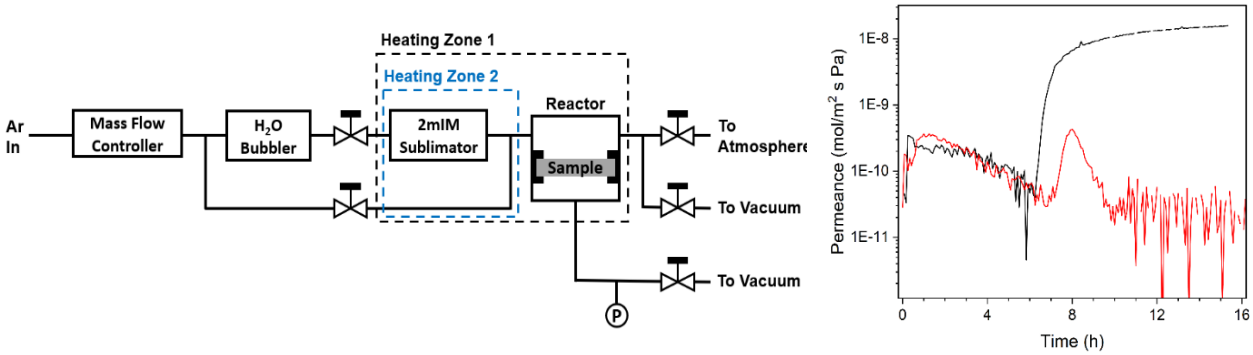

Figure 10. Schematic of Flow Reactor for *In Situ* Monitoring of Permeation During Imidazolate Vapor Treatments. Equipment and available flow paths in reactor are shown. Permeance as a function of time for two membranes during LIPS treatment (transformation of impermeable ZnO deposit to permeable membrane).

Computational Studies In support of the experimental characterization efforts, computational approaches have been utilized to assess the enthalpic costs of ZIF-8 framework distortions, to determine vibrational spectra of ZIF-8 structures without and with adsorbed guest molecules, and to obtain adsorption isotherms for a variety of compounds of interest to separation applications. **Figure 11** shows unary and binary adsorption isotherms for three systems: *n*-butane/2-methylpropane, propanal/acetone, and propan-1-ol/propan-2-ol.

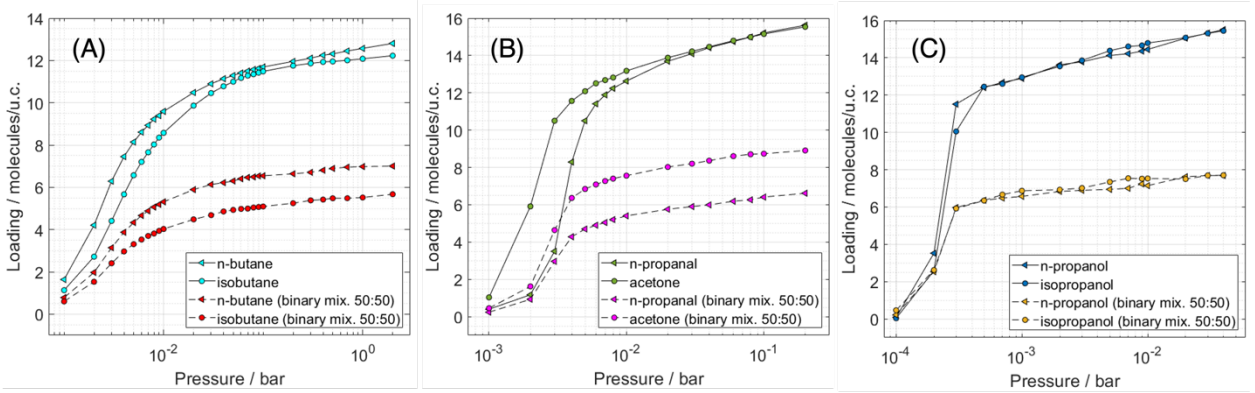

Figure 11. Simulated unary and binary adsorption isotherms in defect-free ZIF-8 for (A) n-butane/2-methylpropane, (B) propanal/acetone, and (C) propan-1-ol/propan-2-ol at 298 K.

These data were obtained from Gibbs ensemble Monte Carlo simulations using force fields taken from the literature. For these three isomer pairs, the saturation loadings obtained from unary isotherms do not yield any pronounced difference between the linear and branched isomers, as one would also expect from the very similar molar volumes in the liquid phase. Interestingly, the positions of the inflection point in the isotherms are not simply related to differences in the saturated vapor pressure. Simulations of the binary mixtures indicate departures from ideal adsorbed solution theory for *n*-butane/2-methylpropane, and propanal/acetone, whereas the alcohol mixture behaves very close to ideal. The reason is that these alcohols form hydrogen-bond moieties in the ZIF-8 cages with the OH groups near the cage center and the alkyl tails oriented toward the hydrophobic ZIF-8 walls. For the butane isomer mixture, adsorption favors n-butane with the selectivity ranging from 1.3 to 1.7, and the selectivity persists at high loading despite the very similar saturation loadings for the individual compounds. In contrast, for the C_3H_6O isomers, adsorption favors acetone, the isomer with the branched structure, with the selectivity ranging from 1.4 to 2.0. Due to the nearly spherical cage, defect-free ZIF-8 does not yield large adsorption selectivities for these pairs. Part of the motivation for these adsorption studies was to find molecules that would be suitable for IRRAS experiments probing adsorption in thin films.

We also used first-principles molecular dynamics simulations to compute vibrational spectra to aid the interpretation of the IRRAS experiments. In particular, for the partially disordered ZIF-8 samples assignment of new features appearing in the spectra requires finding model structures that reproduce these new features and, hence, allow to connect IR peaks to structural features. Examples of these calculations are presented below.

Thin Film Adsorption Using IRRAS In addition to tracking the *in situ* plasma modification of ZIF-8 films, IRRAS was used to follow adsorption and desorption of various molecules on ZIF-8 thin films (thickness ca. 150 nm), supported on Au-coated Si substrates, that were synthesized using the LIPS method. In IRRAS, modulation of the polarization of incident light can be used to eliminate the gas phase components in the spectra, so that only modes corresponding to surface-bound species are visible. These molecules included propane, propene, propanol, isopropanol, and acetonitrile. The first four molecules in this list provided useful preliminary data but had the difficulty of their vibrational modes overlapping with framework phonon vibrations. Unpublished loading vs pressure data for propane is shown in **Figure 12**, based on a

strong vibrational mode in the ~3000 cm^{-1} region, corresponding to (-CH_3) and Methylene (-CH_2) stretching modes. This figure shows the comparison of our isotherms of propane obtained from simulations and IRRAS (black and red points, respectively), with the isotherms reported in the literature (blue points) close to room temperature. In our experiments (red stars in the figure), the ZIF-8 film was exposed to different pressures of propane at 300 K and IR spectra were acquired in parallel using both s-polarized and p-polarized light at each pressure point to prepare adsorption isotherms.

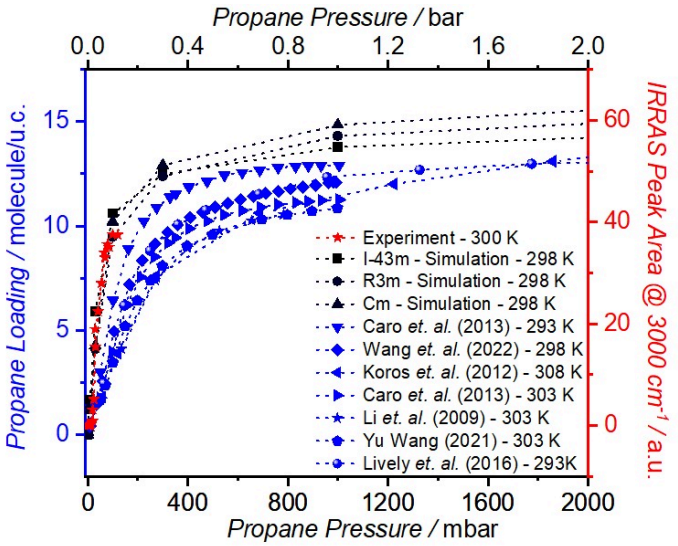

Figure 12. Propane adsorption isotherms in ZIF-8 near room temperature. Blue symbols correspond to literature data, while black symbols correspond to our simulations, and red to experimental data using infrared reflection absorption spectroscopy (IRRAS).

For simulations, three different structure types of ZIF-8 were considered (black symbols in the figure), the more commonly used I-43m, as well as R3m and Cm. *NpT* Gibbs ensemble Monte Carlo simulations were carried out to obtain the adsorption loading and the isotherms. At about 1 bar, we see the saturation of all the reported propane adsorption isotherms in ZIF-8. Due to technical system limitations, the higher-pressure range is not accessible in the IRRAS chamber.

To get a cleaner picture of the adsorption process, and to correlate changes from adsorbate modes with changes in framework modes, we carried out experiments with acetonitrile (ACN), for which the CN stretching vibrational mode (2200+ cm^{-1}) does not overlap with any of the framework modes. Difference spectra (using ultra high vacuum as a reference spectrum) as a function of pressure are shown in **Figure 13**, for a range between 0.001 and 3 mbar. The corresponding simulated difference spectra is shown in red at the bottom of the same figure. As the adsorption of ACN progresses as evident by the 2204 cm^{-1} peak, a ZIF-8 peak at 1585 cm^{-1} is attenuated. From simulated ZIF-8 IR spectra (see below), it is known that this peak is not present in defect free frameworks, but it is present when the structure is missing a Zn linker. This suggests that it is this defect within the experimental structure that the ACN molecules interact with during adsorption at this pressure range. Interactions with non-defective parts of the framework are expected at higher pressures, conditions at which

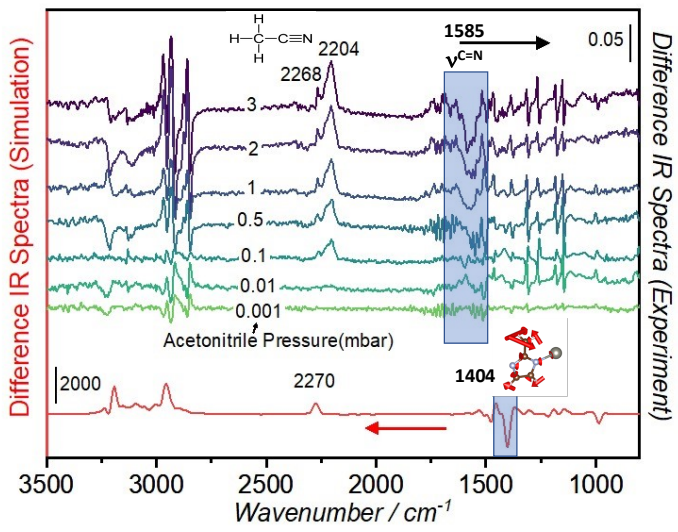

Figure 13. Top: experimental IRRA difference spectra for acetonitrile adsorption on a ZIF-8 thin film at increasing pressures, using as a reference the spectrum in ultra-high vacuum. Bottom: simulated difference IR spectrum for a loading of 12 molecules per unit cell.

a phonon mode in the 1400+ cm^{-1} region would be affected according to the simulations (simulated loading of 12 molecules per unit cell).

The correlation of changes between adsorbate and framework vibrational modes during the adsorption process, by *in situ* IRRAS studies, provides a powerful tool to reach a better fundamental understanding of the mechanistic aspects of this process. This is particularly true when these correlations are supported by simulations using various possible framework configurations (including the presence of defects). However, to properly identify the parts of the framework participating in the adsorption process, a good understanding of the assignments of the spectral features was needed. A thorough literature review of these assignments revealed discrepancies in various publications that needed to be settled. **Figure 14** shows the resulting assignments based on comparing experimental, simulated, and literature data. This was used for example in the analysis of **Figure 13** to correlate the interaction of ACN with C=N groups resulting from missing Zn defects based on the concomitant changes (adsorbate and framework) in the spectra.

These results demonstrate that determination of adsorption properties and identification of defects in thin ZIF films can be accomplished by a combination of IRRA spectroscopy and simulations of adsorption isotherms and vibrational spectra.

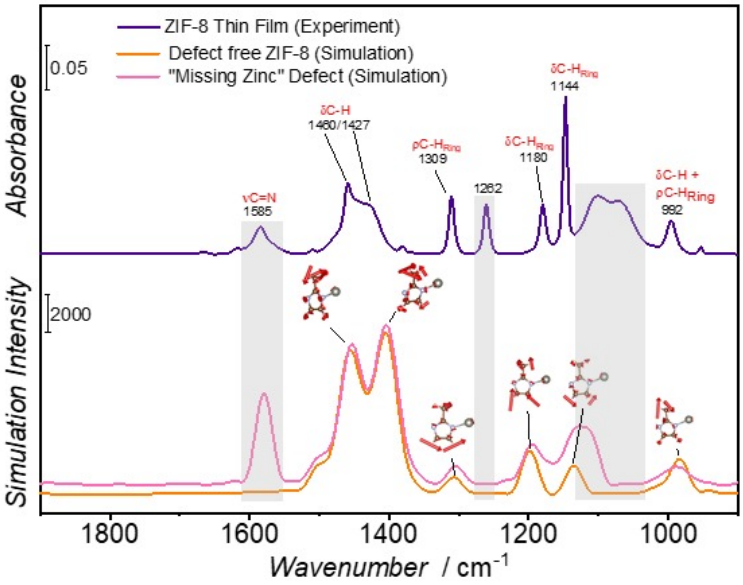

Figure 14. Peak assignments for ZIF-8 framework phonon vibrations as well as schematics showing the active part of the structure involved in such vibration, using vectors to illustrate the magnitude of the motion of each atom. The top spectrum (purple) is an experimental measurement of an as-prepared ZIF-8 film, while the bottom two spectra correspond to simulations of a defect-free structure (orange) and missing-Zn-defect structure (pink). Peaks that are assigned to defects (e.g., missing zinc atoms from the framework) and a peak present in experiments at 1260 cm^{-1} that is currently unidentified from simulations are highlighted in grey.

Publications / Accepted Manuscripts

[1] Hayashi, M., Lee, D. T., de Mello, M. D., Boscoboinik, J. A. & Tsapatsis, M. ZIF-8 Membrane Permselectivity Modification by Manganese(II) Acetylacetonate Vapor Treatment. *Angew. Chem. Int. Ed.* **60**, 9316-9320, doi:10.1002/anie.202100173 (2021).

[2] Miao, Y. R., Lee, D. T., de Mello, M. D., Abdel-Rahman, M. K., Corkery, P., Boscoboinik, J. A., Fairbrother, D. H. & Tsapatsis, M. Electron beam induced modification of ZIF-8 membrane permeation properties. *Chem. Commun.* **57**, 5250-5253, doi:10.1039/d1cc00252j (2021).

[3] Zhuang, L., Corkery, P., Lee, D. T., Lee, S., Kooshkbaghi, M., Xu, Z.-l., Dai, G., Kevrekidis, I. G. & Tsapatsis, M. Numerical simulation of atomic layer deposition for thin deposit formation in a mesoporous substrate. *AIChE J.* **67**, e17305, doi:10.1002/aic.17305 (2021).

[4] Lee, D. T., Corkery, P., Park, S., Jeong, H.-K. & Tsapatsis, M. Zeolitic Imidazolate Framework Membranes: Novel Synthesis Methods and Progress Toward Industrial Use. *Annu. Rev. Chem. Biomol.* **13**, 529-555, doi:10.1146/annurev-chembioeng-092320-120148 (2022).

[5] Miao, Y. R., Lee, D. T., de Mello, M. D., Ahmad, M., Abdel-Rahman, M. K., Eckhert, P. M., Boscoboinik, J. A., Fairbrother, D. H. & Tsapatsis, M. Solvent-free bottom-up patterning of zeolitic imidazolate frameworks. *Nat. Commun.* **13**, 420, doi:10.1038/s41467-022-28050-z (2022).

[6] Dorneles de Mello, M., Ahmad, M., Lee, D. T., Dimitrakellis, P., Miao, Y., Zheng, W., Nykypanchuk, D., Vlachos, D. G., Tsapatsis, M. & Boscoboinik, J. A. In Situ Tracking of Nonthermal Plasma Etching of ZIF-8 Films. *ACS Appl. Mater. Interfaces* **14**, 19023-19030, doi:10.1021/acsami.2c00259 (2022).

[7] Gu, H., Lee, D. T., Corkery, P., Miao, Y., Kim, J.-S., Yuan, Y., Xu, Z.-l., Dai, G., Parsons, G. N., Kevrekidis, I. G., Zhuang, L. & Tsapatsis, M. Modeling of deposit formation in mesoporous substrates via atomic layer deposition: Insights from pore-scale simulation. *AIChE J.* **68**, e17889, doi:10.1002/aic.17889 (2022).

[8] Patel, R., Castro, J., Tsapatsis, M. & Siepmann, J. I. Molecular Simulations Probing the Adsorption and Diffusion of Ammonia, Nitrogen, Hydrogen, and Their Mixtures in Bulk MFI Zeolite and MFI Nanosheets at High Temperature and Pressure. *J. Chem. Eng. Data* **67**, 1779-1791, doi:10.1021/acs.jced.2c00086 (2022).

[9] Yuan, Y., Ping, H., Lee, D. T., Corkery, P., Zhang, Z., Xue, S.-M., Zhuang, L. & Tsapatsis, M. CFD Simulation of the Dosing Behavior within the Atomic Layer Deposition Feeding System. *Ind. Eng. Chem. Res.*. **62**, 9335-9347, doi:10.1021/acs.iecr.3c01151 (2023).